Figure 7

B.1 B.2

Distribution of pPB-HSA in normal rats. Immunohistochemical detection of pPB-HSA (B1) in the liver using anti-HSA antibodies. NTCP staining demonstrates the localization of hepatocytes (B2). Original magnification 200x. n=3

Figure 8

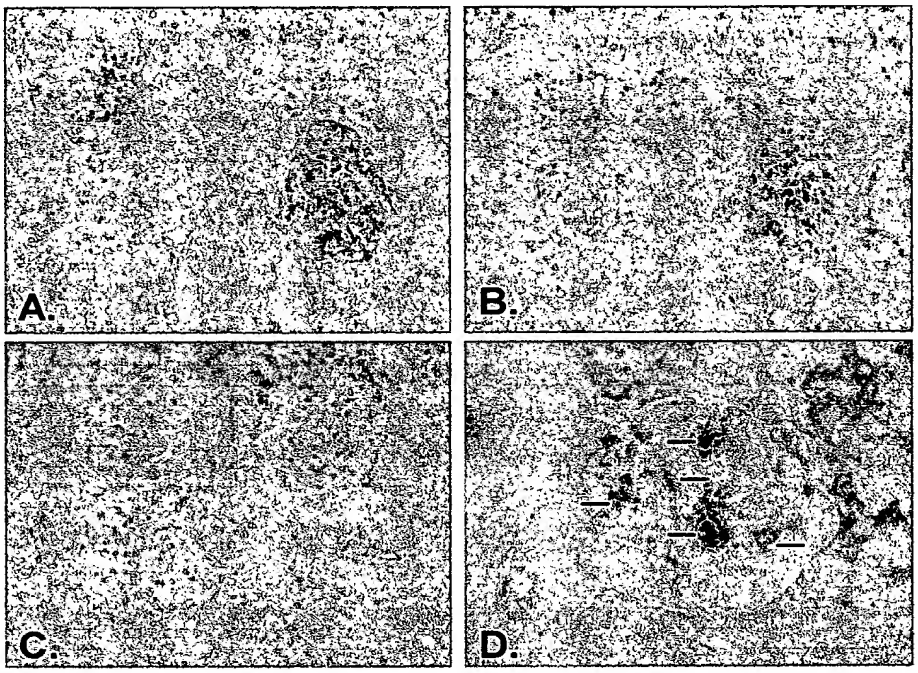

Figure 8. Fig. A.: The renal localisation of the PDGF-β receptor in rats with kidney fibrosis at 21 days after i.v. injection of anti-Thy1.1 IgG. Fig. B and C: Immunohistochemical staining for HSA in these fibrotic rats receiving pPB-HSA (B) or HSA (C) at 10 min after i.v. administration. Note that in glomeruli with a higher expression of PDGF-β receptor, more uptake of pPB-HSA was found (fig. A and B are consecutive sections showing the same glomeruli). Fig. D. Co-localisation of pPB-HSA (red staining) with α–smooth muscle actin positive cells (blue staining) as indicated by arrows. Original magnifications 200x (fig A-C), and 400x (fig. D).

Figure 9

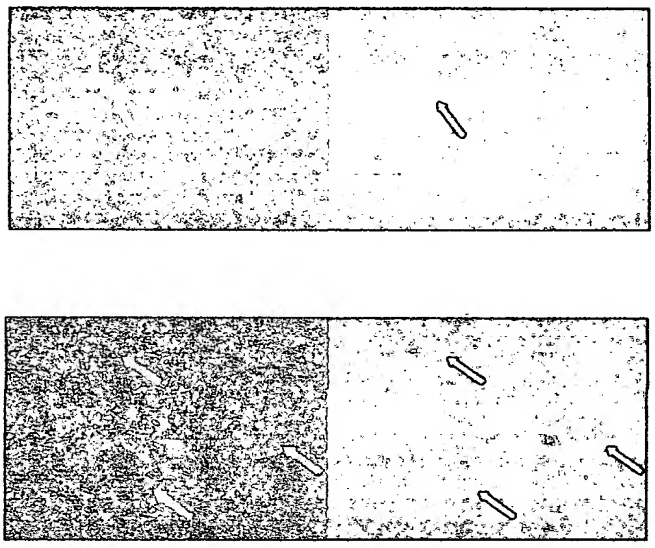

Intrarenal accumulation of DiI-labeled liposomes in normal rat kidneys (Fig. A) and 7 days after induction of glomerulonephritis (Anti-Thy1 nephritis; Fig. B). pPB-HSA, recognizing the PDGF-receptor, was incorporated in these liposomes according to standard procedures. Anti-Thy1 nephritis is characterized by increased receptor expression for PDGF after day 4. Left pictures depicts lightmicroscopical staining, right picture fluorescence staining. Arrows indicate glomeruli. Not the absence of fluorescence in normal rats, and the abundant staining for modified liposomes during anti-Thy1 nephritis.

Figure 10

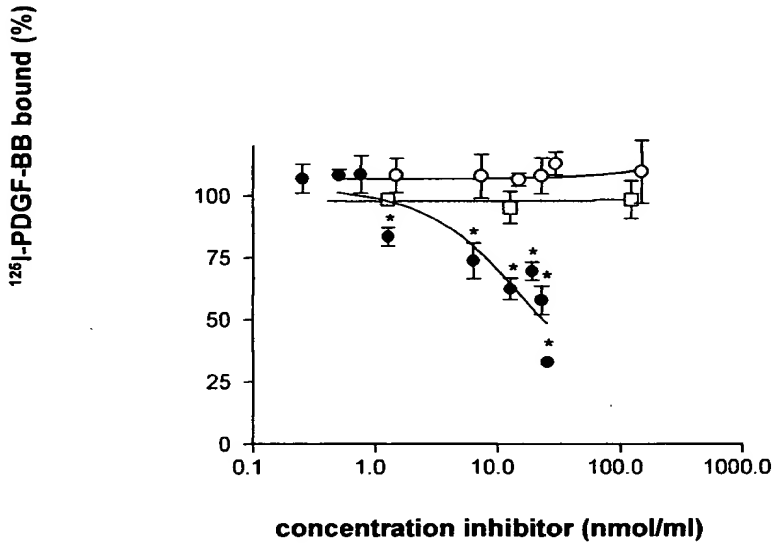

Binding of PDGF-BB (^{125}I labelled) to the PDGF receptors in confluent cultures of NIH/3T3 fibroblasts in the presence of pPB-HSA (●, 0-25 μM), HSA (○, 0-150 μM), or cyclic peptide pPB (□, 0-250 μM). Of note, only in the presence of pPB-HSA, binding of ^{125}I-PDGF-BB to the cells is inhibited (* $p<0.05$). Results are expressed as the mean±SEM (n=3).

Figure 11(a)

Construction of a fusion protein recognising both adenoviral type 5 fiber knob and PDGFβ-receptor which is highly expressed on activated stellate cells. Schematic representation of the gene targeting approach to activated stellate cells. Adenovirus is coated with CSRNLIDC-S11 fusion protein blocking binding to its native receptor CAR.

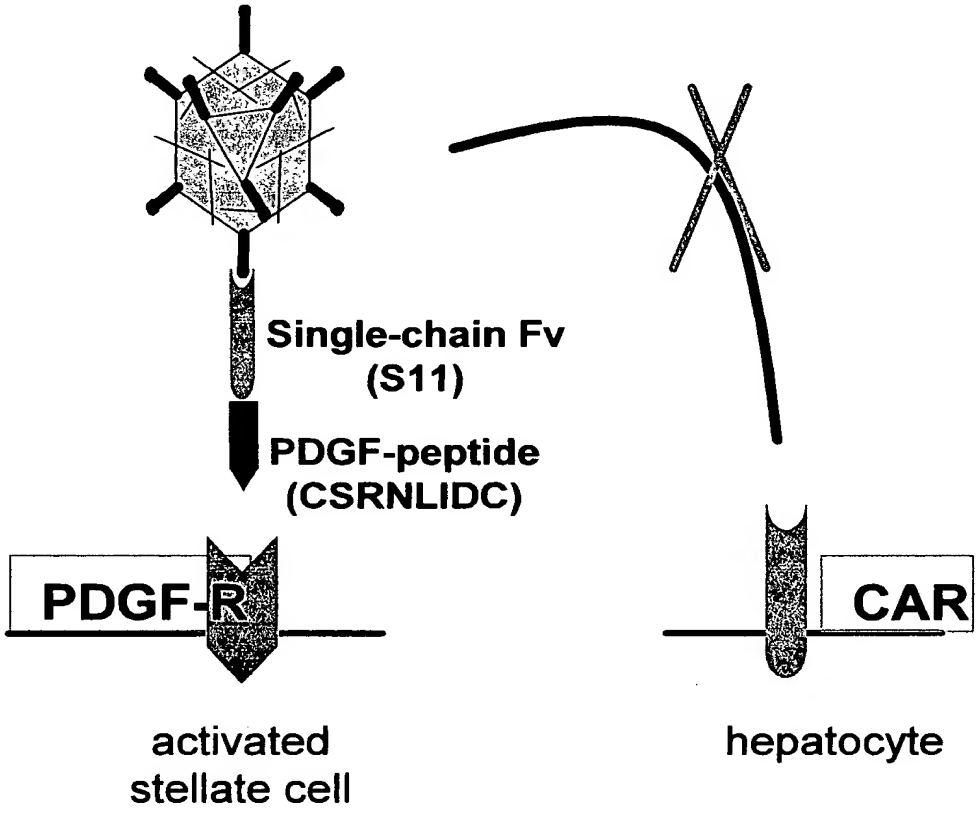

Figure 11(b)

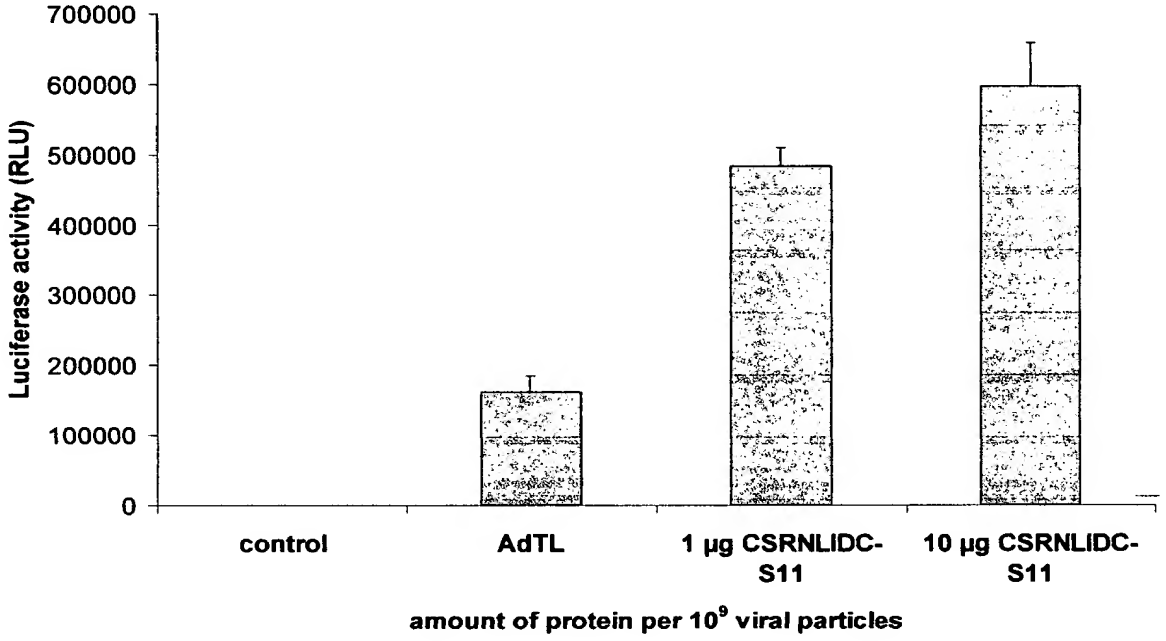

CSRNLIDC-S11 increases adenoviral gene transfer in activated rat stellate cells. Culture-activated stellate cells were infected with PDGF-receptor retargeted adenovirus. A ratio of 1 or 10 µg of CSRNLIDC-S11 per 10^9 viral particles of AdTL was used. Activated stellate cells were infected with an MOI of 10. Gene transfer is presented as luciferase activity (relative light units) measured 48 hours after infection. Representative data of 3 independent stellate cell isolations are shown with the mean of n = 3 per condition.